

# Uplink resource management in 5G: when a distributed and energy-efficient solution meets power and QoS constraints

A. Grassi *Student Member, IEEE*, G. Piro, *Member, IEEE*, G. Bacci, *Member, IEEE*,  
and G. Boggia, *Senior Member, IEEE*

**Abstract**—Massive Multiple-Input Multiple-Output (mMIMO) is emerging as a cornerstone technology for 5G communications. It promises to scale up the performance of the conventional communication systems by growing the number of antennas at the base station side. This paper proposes a decentralized, scalable, and energy efficient radio resource allocation method tailored for the uplink of the upcoming 5G air interface, based on the mMIMO physical layer. The proposed solution elaborates on a game-theoretical approach, which aims at maximizing the energy efficiency of mobile terminals, while guaranteeing the respect of average data rates and power consumptions constraints. This formulation leads to a low-complexity, iterative, and distributed algorithm, which considers (just to mention few relevant issues) the impact of channel time selectivity, delayed feedback from the base station, and physical-layer details of the selected communication technology. An extensive simulation campaign, considering a LTE-A-based multicellular system based on mMIMO, is used to evaluate the benefits of the proposed technique. By calculating energy efficiency, user and peak data rates, spectral efficiency, outage probability, and other minor performance indexes, the reported results clearly demonstrate the performance gain that the designed solution offers with respect to baseline strategies.

**Index Terms**—5G, energy efficiency, massive MIMO, distributed algorithms, game theory.

## I. INTRODUCTION

IT is evident to everyone that the mobile Internet is experiencing a very fast growth thanks to the increasing demand for pervasive video and broadcast-like services, broadband access capabilities everywhere, seamless connectivity with a high user speed, massive Internet of Things applications, and extreme real-time, lifeline, and ultra-reliable communications. This will bring to a 1000-fold increment of overall mobile data traffic by 2020 [1], [2]. But, 4th generation mobile networks, i.e., Long-Term Evolution (LTE) and LTE-Advanced (LTE-A) technologies, are not able to support the requirements of upcoming mobile applications. Therefore, a lot of effort from research community is devoted for the design of 5th Generation (5G) wireless technologies that should address

high spectral efficiency, very low latencies, and limited power consumptions [3]–[6].

Since the LTE release 8, Multiple-Input Multiple-Output (MIMO) has been considered as a key technology innovation, able to improve the performance of the cellular system [7]. With the LTE release 10, new transmission schemes have been standardized to further increase data throughput and spectral efficiency. With reference to the uplink, Multi-User MIMO (MU-MIMO) was introduced to allow multiple users (up to 8) to concurrently transmit different data streams by using the same set of time-frequency resources [8]. Today, many contributions in the literature share the opinion that adopting a higher amount of base station antennas may improve MU-MIMO capabilities, thus providing huge capacity gains with respect to conventional communication systems. This trend is converging towards the definition of a new cornerstone technology for the 5G: the Massive Multiple-Input Multiple-Output (mMIMO) [9].

With mMIMO, radio resource management becomes even more challenging. From one side, mMIMO permits to serve multiple users concurrently. In fact, it benefits from the multi-user diversity to effectively separate many data streams overlapped in the time-frequency domain. From another side, when the same set of resources is jointly allocated to an excessive number of users, the overall performance level may significantly decrease. Therefore, depending on the target performance index that needs to be optimized (the peak throughput or the user fairness, for instance), specific methodologies should be designed for both downlink [10]–[13] and uplink [14].

Energy efficiency is another relevant aspect for the 5G: it is expected that future cellular networks should be able to reduce current power consumptions as much as possible [15], while targeting an energy saving up to 50% [16]. Although there is a lot of work in the literature on the subject of energy efficiency (e.g. see [17]–[19]), this goal becomes particularly challenging for the uplink, where it is extremely important to increase the battery life of mobile terminals [20], [21]. In this context, game theory [22] could be applied to solve energy efficiency maximization problems [23]–[25]. For instance, the work in [26] presents a decentralized radio resource allocation algorithm, elaborated on a game-theoretical approach that aims at maximizing the energy efficiency of mobile terminals. Unfortunately, the designed solution has many limitations: (i) it assumes ideal (i.e., time-invariant)

Copyright (c) 2015 IEEE. Personal use of this material is permitted. However, permission to use this material for any other purposes must be obtained from the IEEE by sending a request to pubs-permissions@ieee.org.

A. Grassi, G. Piro, and G. Boggia are with the Dept. of Electrical and Information Engineering (DEI), Politecnico di Bari, v. Orabona 4, 70125, Bari, Italy; e-mail: {alessandro.grassi, giuseppe.piro, gennaro.boggia}@poliba.it.

G. Bacci is with M.B.I. srl, Via F. Squartini, 7 - 56121 Pisa, Italy. e-mail: gbacci@mbigroup.it

channel conditions; (ii) it does not consider any constraint for the maximum transmission power; (iii) it evaluates the channel capacity through the Shannon formula, and (iv) it supposes an instantaneous Channel Quality Indicator (CQI) reporting scheme. Furthermore, it also proposes a simple performance evaluation, which does not offer any comparison with other baseline strategies. Thus, the contribution discussed in [26] does not appear mature enough for being directly adopted in a real technology.

Based on this analysis, this paper intends to significantly extend the work proposed in [26], by designing and evaluating a more complete radio resource allocation method, that deals with all the details characterizing uplink communications in mMIMO-based 5G systems. Similarly to [26], it elaborates on a game-theoretical approach (specifically, a non-cooperative game) that aims at maximizing the energy efficiency of mobile terminals. Nevertheless, the novel approach discussed herein jointly considers the respect of average data rates and power consumptions constraints. Moreover, differently from [26], it clearly addresses time-variant channel conditions, realistic system capacity and transmission interfaces based on the LTE-A technology, users' speed, CQI delay, and a higher number of base station antennas allowing the management of multiple concurrent uplink data streams. The resulting low-complexity, iterative, and distributed algorithm allows mobile terminals to autonomously select their uplink transmission settings, including the set of sub-channels to use for the transmission, the Modulation and Coding Scheme, and the power profile.

The performance of the proposed algorithm is evaluated through the LTE-Sim tool [27]. Simulations consider multi-user and multi-cell environments, and evaluate the impact of the number of users, the user speed, and the target data rate on the overall system performance. To further demonstrate the effectiveness of the designed solution, we compare it with other baseline radio resource management techniques built on top of the mMIMO physical layer, namely *proportional fair* and *multi-user mMIMO* schemes. Obtained results show that the proposed approach outperforms the baseline strategies by offering higher energy efficiency and acceptable spectral efficiency and outage probability.

The rest of the paper is organized as follows. The state of the art on mMIMO and energy efficient transmission schemes is presented in Sec. II. The proposed theoretical approach and the simulation results are discussed in Sec. III and Sec. IV, respectively. Finally, Sec. V draws the conclusions and presents some possible future directions for this work.

## II. STATE OF THE ART

Today, mMIMO is considered as a cornerstone technology for 5G [9], [28]. It aims at scaling up the performance of the conventional MIMO by growing the number of antennas at the base station side (i.e., it can be equal to tens or hundreds) [29]. With more transmitting antennas, it is possible to jointly enable transmit/receive diversity, spatial multiplexing, and beam-forming.

In summary, mMIMO offers: (i) the ability to break down the effect of fast fading as it is averaged over a large number

of signals [30]; (ii) the adoption of simpler transmission and receive processing techniques like Maximum Ratio Transmission (MRT) and Maximum Ratio Combining (MRC), which are able to guarantee similar performance compared to more complex receivers based on the powerful Minimum Mean-Square Error (MMSE) and Regularized Zero Forcing (RZF) schemes [31]; and (iii) the minimization of typical issues of the radio link, like interference, channel estimation errors, and noise [9].

Moreover, mMIMO has an important impact on power demands. Some studies highlight that the radiated power goes to zero as the number of antennas  $N$  increases towards infinity [9], [30]. Specifically, it can be inversely proportional to  $N$  when perfect Channel State Information (CSI) is available, and to  $\sqrt{N}$  with imperfect CSI. The amount of power required by the electronic circuitry, instead, increases with the number of antennas. According to [32]–[35], the number of base station antennas could be properly set as a function of some target performance indexes (including the energy efficiency) and system assumptions.

In the downlink, the simplest way to deal with mMIMO is to allocate the entire bandwidth to all active users. Then, linear precoding techniques, like MRC or ZF, are used by mobile terminals to decode their own data streams with very limited intra-cell interference. Of course, other optimized approaches have been proposed in the literature. In [10], the problem of maximizing the energy efficiency of a mMIMO system is formulated as a non-convex optimization problem and solved using an iterative algorithm based on fractional programming. The maximization of the peak data rate is addressed in [11], which derives a method that combines wide-band analog beam-forming and a per-subcarrier digital beam-forming, and takes into account per-subcarrier power constraints. Some other schemes involve cooperation among multiple cells to reach user fairness [12] and load balancing [13].

As already anticipated in Sec. I, radio resource allocation and energy efficiency are even more challenging for the uplink. An algorithm that maximizes only the spectral efficiency is presented in [14]. Specifically, the work evaluates the system capacity by considering both the infinite-antennas regime (derived analytically) and the finite-antennas regime (through simulations). In [20], instead, energy efficiency is the objective function, to be optimized as a function of the number of antennas at the base station and the user data rate. In this case, however, Quality-of-Service (QoS) constraints are not considered and the allocation of the whole bandwidth for all users (likewise the baseline approach for the downlink) is still assumed. In [21], the total transmission power is minimized via uplink power control, while guaranteeing a minimum Signal-to-Interference-plus-Noise Ratio (SINR) and a maximum per-user power. Yet, the assumption of full-bandwidth transmissions remains. In some cases, game theory is used to develop distributed and optimized resource management schemes in wireless networks [23]. For example, non-cooperative games are formulated in [24], [25], and [26] for different purposes. The approach described in [24] aims at maximizing the user data rate in a MIMO system, while respecting power constraints. The solution proposed in [25]

Table I: Comparison among our work and the other solutions focusing on uplink mMIMO

Features	[14]	[20]	[21]	[24]	[25]	[26]	Our work
Maximization of energy efficiency		✓	✓		✓	✓	✓
Respect of QoS constraints			✓		✓	✓	✓
Respect of power constraints			✓	✓	✓		✓
Distributed approach				✓	✓	✓	✓
Game-theoretical approach				✓	✓	✓	✓
Power control in the frequency domain				✓		✓	✓
Technology-driven design							✓

focuses on mMIMO and addresses the optimization of the uplink energy efficiency by properly distributing the transmission power between data and pilot signals, while taking into account the minimum SINR experienced by each mobile terminal and the maximum available transmission power. It, however, leverages a simple MRC receiver and assumes a full-band and flat power allocation. Conversely, [26] presents a decentralized radio resource allocation algorithm that aims at maximizing the energy efficiency of mobile terminals by properly modulating the transmission power in the frequency domain. Discarding the commonly used flat power transmission, the work in [26] promises to increase system capacity by better reacting to inter-user interference. Unfortunately, it still presents many limitations that prevent a direct adoption in a real technology (see Sec. III-B for more details).

As already anticipated in Sec. I, this paper proposes a novel radio resource allocation approach, which overcomes all the aforementioned issues. In particular, starting from the approach designed in [26], a more complete solution dealing with technological details available in a real scenario (e.g., *technology-driven design*) is developed. The main differences among our work and the other solutions described before are summarized in Table I.

### III. PROPOSED SCHEME

In this section, we describe the proposed resource allocation scheme, suitable for the upcoming 5G air interface based on the mMIMO physical layer. It is used to handle uplink communications in a fully distributed and energy-efficient way, while ensuring QoS requirements and power constraints.

Apart from the huge number of base station antennas offered by mMIMO, the considered physical layer is based on LTE-A specifications. As well known, in the LTE-A technology, resources are allocated in the time/frequency domain. Considering only the time domain, they are distributed every Transmission Time Interval (TTI), each one made up by two time-slots lasting 0.5 ms. The total bandwidth is divided in sub-channels of 180 kHz. A time/frequency radio resource spanning over one time-slot in the time domain and over one sub-channel in the frequency domain is called a Resource Block (RB), which corresponds to the smallest radio resource unit that can be assigned to a user for data transmission.

The allocation of radio resources is a centralized task executed by the packet scheduler at the base station side [36], [37]. When mMIMO is used, multiple users can be concurrently scheduled. However, radio resources are still allocated by the base station in a centralized fashion.

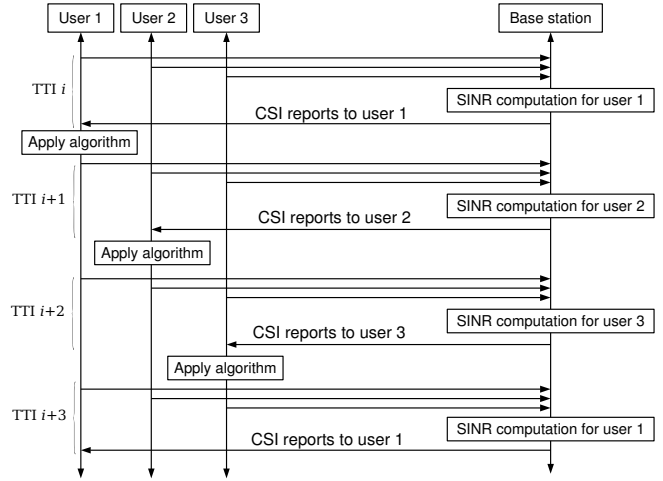


Fig. 1: Graphical representation of the update sequence.

On the contrary, our proposal introduces a fully distributed solution where all the users may transmit data at the same time by (potentially) using the whole set of frequencies assigned to a given cell and without the need for a centralized control at the base station. Bypassing the role of the packet scheduler, each user autonomously determines the set of sub-channels to use for the transmission, the Modulation and Coding Scheme (MCS), and the power profile in the frequency domain. To this aim, a non-cooperative game is implemented, whose goal is to solve an optimization problem, maximizing the energy efficiency under the constraints of both QoS requirements and maximum transmission power. In this scheme, the base station is just in charge of measuring the channel quality for each uplink connection, i.e., the Channel State Information (CSI), and feeding it back to users through downlink control messages.

It is important to note that it is not recommended that two or more users update their transmission settings (and in particular their power profiles) simultaneously. In fact, if multiple users perform these choices at the same time, they may not take into account the interference level produced by concurrent transmissions, thus making the entire procedure unstable. To avoid this issue, users apply the proposed algorithm one by one, based on the feedback provided by the base station. As depicted in Fig. 1, the base station sends one CSI report at a time and the user can implement the algorithm only if it is the recipient of the aforementioned report. Otherwise, it will send data by using transmission settings already selected in the past. The base station can select the user to send the CSI report to by simply adopting the Round Robin method.

To ease the comprehension of the notions presented in the following, a summary of symbols is reported in Table II.

#### A. Problem description

The reference scenario is a multi-cell system where cells share the same spectrum composed by  $B$  consecutive sub-channels. Let  $\mathcal{B} = \{0, 1, \dots, B - 1\}$  be the set of these sub-

Table II: List of mathematical symbols

symbol	description
$b$	sub-channel index
$B$	total number of sub-channels
$\mathcal{B}$	set of available sub-channels
$C_{i,u,b}$	channel capacity of user $u$ on sub-channel $b$ during TTI $i$
$E_{i,u}$	energy efficiency during TTI $i$ for user $u$
$\mathbf{h}_{i,u,b}$	vector of channel gains from user $u$ to its base station on sub-channel $b$ during TTI $i$
$M$	number of receiving antennas at the base station
$N_0$	thermal noise power
$O_u$	target bit-rate of user $u$
$P_M$	maximum allowed power for each mobile user
$R_{i,u}$	bit-rate achieved during TTI $i$ for user $u$
$S$	number of sub-channels used to calculate the effective SINR $\Gamma_{i,u}^{\text{eff}}$
$S$	subset of sub-channels used to calculate the effective SINR $\Gamma_{i,u}^{\text{eff}}$
$u$	user index
$\mathcal{U}$	set of available users
$U$	total number of users
$i$	TTI index
$\Gamma_{i,u}(b)$	SINR that user $u$ gets on sub-channel $b$ during TTI $i$
$\Gamma_{i,u}^{\text{eff}}$	effective SINR of user $u$ on all sub-channels during TTI $i$
$\Delta f$	sub-channel spacing in the frequency domain
$\lambda_{i,u}^a$	waterfilling level for maximum energy efficiency of user $u$ during TTI $i$
$\lambda_{i,u}^b$	waterfilling level for minimum bit-rate of user $u$ during TTI $i$
$\lambda_{i,u}^c$	waterfilling level for maximum power of user $u$ during TTI $i$
$\lambda_{i,u}^*$	final waterfilling level for user $u$ during TTI $i$
$\Pi_{i,u,b}$	transmission power level used by user $u$ on sub-channel $b$ during TTI $i$
$\tilde{\Pi}$	mobile terminal non-radiative power
$\mathbf{\Pi}_{i,u}$	power profile used by user $u$ during TTI $i$
$\mathbf{\Pi}_{i,u}^*$	optimal power profile used by user $u$ during TTI $i$

channels available in every cell, each one with spacing  $\Delta f$ .<sup>1</sup>

The set of users available in a given cell of the scenario are denoted by  $\mathcal{U} = \{0, 1, \dots, U-1\}$ , where  $U = |\mathcal{U}|$  is the total number of users.

During the  $i$ -th TTI, a user  $u$  may transmit its data by (potentially) using the whole set of frequencies available in the cell (according to the multi-user transmission capability offered by mMIMO, however, many users can send packets by using the same set of radio resources). The power level in each sub-channel  $b \in \mathcal{B}$  is equal to  $\Pi_{i,u}(b)$ . Therefore, the power profile of user  $u$  during TTI  $i$  is denoted by  $\mathbf{\Pi}_{i,u} = \{\Pi_{i,u}(0); \Pi_{i,u}(1); \dots, \Pi_{i,u}(B-1)\}$ . In this contribution, we also assumed that the total power level that each user can use for the transmission is limited to a given value  $P_M$ .

Also,  $R_{i,u}$  represents the bit-rate of the user  $u$  during TTI  $i$ . Note that, according to the LTE-A behaviour, its value depends on the selected MCS scheme and on the amount of sub-channels adopted for the transmission. At the application layer, each user  $u \in \mathcal{U}$  is subject to a QoS constraint: the perceived throughput  $R_{i,u}$ , averaged over the time interval  $i$ ,

<sup>1</sup>For LTE-A,  $\Delta f = 180$  kHz; whereas  $B$  varies from 6 to 500 depending on the total bandwidth which ranges from a minimum of 1.4 MHz to a maximum value of 100 MHz.

should not be lower than a target value,  $O_u$ . Note that, if this condition is not met, an *outage condition* occurs.

Moreover, let  $\Gamma_{i,u}(b)$  be the SINR measured by the base station for user  $u$  on sub-channel  $b$  during the TTI  $i$  (further details on how to compute this quantity will be given in Sec. III-C).

In line with [26], the energy efficiency for the user  $u$  during the TTI  $i$  can be defined as the ratio between the bit-rate and the total power used for transmission:

$$E_{i,u} = \frac{R_{i,u}}{\tilde{\Pi} + \sum_{b=0}^{B-1} \Pi_{i,u,b}} \quad (1)$$

where  $\tilde{\Pi}$  accounts for the non-radiative power dissipated in the electronic circuitry of the mobile terminal.<sup>2</sup>

The resource allocation technique formulated in this paper aims at evaluating, for each user, the optimal power profile  $\mathbf{\Pi}_{i,u}^*$  that is able to maximize the energy efficiency, while ensuring both QoS and power constraints. It can be formally expressed, for all  $u \in \mathcal{U}$  and for each TTI  $i$ , through the optimization problem

$$\mathbf{\Pi}_{i,u}^* = \arg \max_{\mathbf{\Pi}_{i,u}} E_{i,u} \quad (2)$$

$$\text{subject to: } R_{i,u} \geq O_u \quad (3)$$

$$\sum_{b=0}^{B-1} \Pi_{i,u}(b) \leq P_M. \quad (4)$$

### B. Inputs from a previous work and emerging issues

In [26], the optimization problem described in (2) is formulated as a *non-cooperative game* between users, where the utility function to maximize is  $E_{i,u}$ . The term *non-cooperative* is used to highlight that no explicit cooperation between users is employed [38]. Nevertheless, the behavior of all active players (i.e., users involved in the game that aim at transmitting data over the same spectrum) is indirectly taken into account with the SINR values  $\Gamma_{i,u}(b), \forall b \in \mathcal{B}$  that are periodically sent by the base station as discussed below.

The solution of the game-theoretic problem is investigated in the form of Generalized Nash Equilibrium (GNE) states [39]. In these states, each user adopts the power allocation profile which maximizes its utility function, given the power allocation profile of all other users. Also, the power allocation profile is expected to remain unchanged if all users keep using the same power profiles, because every deviation would result in a lower utility outcome. Thus, a GNE state is intrinsically stable, as all users will stick to it because they have no convenience in doing otherwise. This property is useful in the context of distributed resources allocation mechanisms, where the stability cannot be guaranteed by a centralized entity. The work presented in [26] demonstrates the existence and uniqueness conditions for GNE states of the aforementioned problem. The iterative method useful to reach such states is also presented.

Now, without demonstrating each single step of the algorithm already discussed in [26], we can summarize that the

<sup>2</sup>In this work, the non-radiative power  $\tilde{\Pi}$  is assumed to be a constant value for all users and all TTIs.

optimal power profile is calculated by each user  $u$  as in the following:

- The set of SINRs  $\Gamma_{i,u}(b), \forall b \in \mathcal{B}$  is received from the serving base station.
- A WaterFilling (WF) formula is used to calculate the power profile. During TTI  $i$ , user  $u$  calculates the power level of the sub-channel  $b$  as:

$$\Pi_{i,u}(b) = \max \left\{ \frac{1}{\lambda_{i,u}^*} - \frac{\Pi_{i-1,u}(b)}{\Gamma_{i-1,u}(b)}; 0 \right\} \quad (5)$$

where  $\lambda_{i,u}^*$  is the water level of the WF operator. Note that in [26] it is proved that a power profile is in a GNE state if and only if it is calculated as in (5).

- The parameter  $\lambda_{i,u}^*$  in (5) is set to  $\lambda_{i,u}^* = \min(\lambda_{i,u}^a, \lambda_{i,u}^b)$ , where  $\lambda_{i,u}^a$  is calculated by solving the optimization problem in (2) without considering the minimum rate constraint and  $\lambda_{i,u}^b$  is calculated by imposing the minimum rate constraint, as in (3). More details about the methodology used for computing both  $\lambda_{i,u}^a$  and  $\lambda_{i,u}^b$  can be found in [26].
- With reference to the constraint described in (3), the achievable transmission bit-rate,  $R_{i,u}$ , with the described power profile, is ideally evaluated through the Shannon theorem:

$$R_{i,u} = \sum_{b=0}^{B-1} \Delta f \cdot \log_2(1 + \Gamma_{i,u}(b)). \quad (6)$$

- The algorithm is repeated multiple times until stability is reached. After that, no further updates are made.

Unfortunately, the aforementioned approach cannot be implemented on top of a real technology due to the presence of some limitations. First, since the optimization problem did not consider the power constraint, the final solution may bring to power levels higher than those really supported by mobile terminals, as well as imposed by normative regulations. Second, a time-invariant channel is considered, which means that the propagation loss used for computing  $\Gamma_{i,u}(b)$  is only influenced by the path loss; on the contrary, fading effects are ignored at all. In these conditions, the WF algorithm is able to reach the stability after a few iterations and, as a consequence, its ability to adapt the power profile to network dynamics (elicited by both channel and application traffic) is not investigated in depth. Third,  $R_{i,u}$  is evaluated without considering any physical details of a real technology. In LTE-A, for instance, the user has to transmit data by using the same MCS for all the selected sub-channels and the achieved bit-rate could be significantly different with respect to the Shannon bound (especially in the presence of intense frequency selective fading). Fourth, it is supposed that each user may potentially transmit over the entire spectrum, even if the achieved bit-rate is higher than the required one. This assumption can produce huge interference levels (and hence lower performance) in high-load scenarios. Finally, the WF algorithm described in (5) assumes that each user receives CSI indicators from the base station every TTI, with no delays. Therefore, the impact that a real protocol may have on CSI reporting delays is completely ignored.

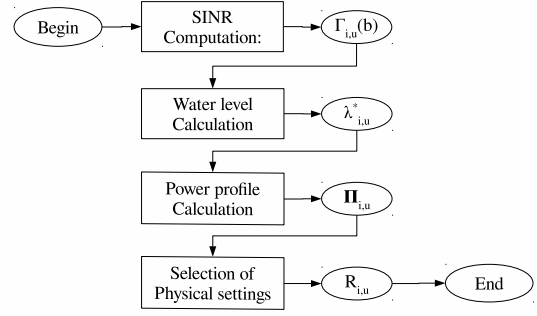


Fig. 2: Algorithm flow chart.

### C. The proposed solution

As already highlighted in Sec. I, the conceived solution extends the work presented in [26] in order to solve all the aforementioned issues, while ensuring at the same time its feasibility in a real environment under the constraints provided by the underlying technology (including physical transmission rate and maximum transmission power).

The set of tasks implemented by each user are reported in Fig. 2. An in-depth discussion is reported below.

1) *SINR computations*: During the  $i$ -th TTI, the base station uses the MMSE receiver for calculating the SINR,  $\Gamma_{i,u}(b)$ , related to the user  $u$  and the sub-channel  $b$  (note that MMSE is used as the baseline decoder in LTE-A) as:

$$\Gamma_{i,u}(b) = \Pi_{i,u}(b) \mathbf{h}_{i,u}^H(b) [N_0 \mathbf{I}_M + \chi_{tot,u}(b)]^{-1} \mathbf{h}_{i,u}(b) \quad (7)$$

where  $\mathbf{h}_{i,u}(b)$  is the array of channel gains from user  $u$  to each antenna of the base station,  $\mathbf{h}_{i,u}^H(b)$  is its Hermitian conjugate,  $N_0$  is the thermal noise power,  $\mathbf{I}_M$  is the  $M \times M$  identity matrix, and:

$$\chi_{tot,u}(b) = \sum_{j=1, j \neq u}^U \Pi_{i,j}(b) \mathbf{h}_{i,j}(b) \mathbf{h}_{i,j}^H(b) \quad (8)$$

is the inter-user interference, which depends on the transmission power levels and channel gains of the other users transmitting on the same sub-channel and in the same TTI.

Without loss of generality, it is assumed that CSI feedbacks estimated by the base station are received by the user after  $\tau$  TTIs from its calculation (i.e.,  $\tau$  represents the CQI reporting delay expressed in TTIs). Therefore, at the beginning of the  $i$ -th TTI, the user considers as input parameters of the algorithm the set of values  $\Gamma_{i-\tau,u}(b), \forall b \in \mathcal{B}$ .

Starting from the received CSI feedbacks, the user can calculate the wideband effective SINR,  $\Gamma_{i,u}^{\text{eff}}$ , as:

$$\Gamma_{i,u}^{\text{eff}} = -\beta \ln \left[ \frac{1}{S} \sum_{b \in \mathcal{B}} \exp \left\{ -\frac{\Gamma_{i-\tau,u}(b)}{\beta} \right\} \right] \quad (9)$$

where  $S$  is the number of sub-channels used to calculate the effective SINR (contained in a subset  $\mathcal{S} \subseteq \mathcal{B}$ ) and  $\beta$  is a scaling factor that takes into account the different MCSs [40].

2) *Calculation of the water level for the WF operator:* Differently from [26],  $\lambda_{i,u}^*$  is obtained as:

$$\lambda_{i,u}^* = \max \left\{ \min \left\{ \lambda_{i,u}^a, \lambda_{i,u}^b \right\}, \lambda_{i,u}^c \right\}, \quad (10)$$

where:

- $\lambda_{i,u}^a$  represents the solution which maximizes the energy efficiency without taking any constraint into account. The calculation method is very similar to [26], with minor changes described in the Appendix.
- $\lambda_{i,u}^b$  is evaluated as the water level that minimizes the transmission power for a given bit-rate value (set to the minimum required rate  $O_u$ ). Unlike [26], where the physical data rate is estimated by the Shannon theorem, in this contribution  $R_{i,u}$  is obtained as a function  $\mathcal{F}(\cdot)$  of the wideband effective SINR and the number of active sub-channels, as:

$$R_{i,u} = \mathcal{F}(\Gamma_{i,u}^{\text{eff}}, S). \quad (11)$$

In this way, all the details of the underlying technology are carefully taken into account. A detailed description of the function  $\mathcal{F}(\cdot)$  can be found in [41].

- $\lambda_{i,u}^c$  is calculated as the water level which maximizes the bit-rate using a fixed total power, which is set to the maximum power  $P_M$  that mobile terminals are allowed to use.

For the sake of clarity, the pseudo-code for the calculation of  $\lambda_{i,u}^a$ ,  $\lambda_{i,u}^b$ , and  $\lambda_{i,u}^c$  is reported in the Appendix.

3) *Evaluation of the optimal power profile:* As a next step of the procedure, the power profile is calculated, although in its preliminary version, through (5). Moreover, it is subsequently revised in order to reduce the interference levels in highly loaded scenarios, as well as prevent from transmitting over sub-channels experiencing peak fading attenuations.

To this end, not all of the available sub-channels are used for the transmission. Indeed, just a subset of them is selected for this purpose through an iterative procedure. First, all the sub-channels are sorted in decreasing order of SINR. Starting from the sub-channel with the highest SINR value, the corresponding effective SINR and the physical data rate  $R_{i,u}$  are obtained using eqs. (9) and (11), respectively. If the resulting bit-rate is already higher than the target rate, then the iteration stops and this single channel is used. If  $R_{i,u} < O_u$ , the calculation is repeated with the best two channels and the bit-rate is checked again. If needed, more channels are added until the required bit-rate  $O_u$  is reached. When the required number of channels is found, the remaining channels are excluded and the correspondig allocated power is set to zero.

The rationale behind the aforementioned sub-channel selection is that a peak fading attenuation experienced in few sub-channels brings to a low wideband effective SINR value, thus providing a limited physical transmission rate. In other words, the weakest sub-channels are a limiting factor for the throughput, so it is preferable to use as few sub-channels

as possible (and choose those with the highest SINR). This issue is not considered in [26], because the sub-channels are assumed to be independent and any additional sub-channel always results in a higher throughput. Also, reducing the number of sub-channels reduces the total power used for transmission and the multi-user interference, allowing more users to transmit simultaneously.

4) *Selection of physical settings:* At the end, the user may finally select the MCS to use for the transmission. This task is done by using the well known strategy widely accepted for the LTE-A technology [27].

#### IV. PERFORMANCE EVALUATION

The performance of the proposed algorithm is tested using the LTE-Sim open source simulator for cellular networks [27].

To further demonstrate the effectiveness of the designed solution, we also provide a comparison with other baseline radio resource management techniques, built on top of the mMIMO physical layer. In particular, *proportional fair* and *multi-user mMIMO* have been considered as reference techniques.

With the proportional fair allocation, the scheduling of uplink resources is fully orchestrated by the base station. In each time interval, and for each user, a scheduling metric is calculated as the ratio between expected physical data rate and the average average throughput achieved during past sub-frames. Then, only the user with the highest metric is selected for transmission during that time interval [36]. The inter-user interference within a single cell is completely absent. At the physical layer, mobile terminals leverage a flat power profile because the maximum allowed power is uniformly distributed in the frequency domain. Moreover, mMIMO is used to guarantee an improved SINR, due to the combination of a higher number of received signals.

Multi-user mMIMO extends the MU-MIMO transmission scheme by assuming the presence of a higher number of base station antennas. It allows all the users to transmit data at the same time, over the same spectrum. The allocation of uplink resources is not controlled anymore by the packet scheduler. Similarly to the proportional fair scheme, multi-user mMIMO also uses a flat power profile. The mMIMO physical layer is in charge of separating all the multiplexed signals.

##### A. Simulation settings

Simulations assume a multi-cell environment with 7 cells arranged on an hexagonal grid. Each cell has a radius of 500 m, with an inter-site distance of 866 m. In each cell, a number of users (ranging from 5 to 25) is randomly distributed over the entire simulation area with uniform probability.

A system bandwidth of 5 MHz is used, in the operating band  $1920 \div 1924.32$  MHz (corresponding to LTE band 1), with a frequency reuse factor of 1. This generates strong inter-cell interference and shows how the proposed solution works in extreme conditions.

An mMIMO physical layer is always considered and the number of antennas at the base station is set to  $M = 32$ .

To take into account the impact of the signal propagation, the 3rd Generation Partnership Project (3GPP) model for urban

Table III: Simulation parameters

parameter	value
cell radius	500 m
number of cells	7
inter-cell distance	866 m
receiver type	MMSE
bandwidth	5 MHz
number of sub-channels $B$	25
operating frequency	1920 – 1924.32 MHz
number of users per cell	{5, 10, 15, 20, 25}
minimum user bit-rate $O_u$	{300, 1000} kb/s
maximum user transmit power	23 dBm
mobile terminal non-radiative power $\tilde{\Pi}$	10 dBm
number of transmit antennas at mobile user	1
user speed	{3, 120} km/h
mobility model	random direction
MIMO configuration	mMIMO with 32 antennas at the base station side
path-loss model	$128.1 + 37.6 \log_{10}(d)$ [dB]
shadowing model	lognormal with 8 dB std. dev.
fast fading model	Jakes' model with 6, 8, 10, or 12 paths
penetration loss	10 dB
number of runs	25
CSI delay	2 ms

macrocells is considered [42]. In addition, other phenomena included are:

- large-scale shadowing, modeled as a log-normal random variable with 0 mean and 8 dB standard deviation [42];
- penetration loss, set to a constant value of 10 dB [42];
- fast fading, introduced as a random variable with Rayleigh distribution, generated using the Jakes' model with 6, 8, 10 or 12 paths [27].

A Block Error Rate (BLER) model based on the Additive White Gaussian Noise (AWGN) channel is taken into account [27]. Each mobile terminal can use a maximum transmit power of  $P_M = 23$  dBm, whereas the non-radiative power is set to a constant value of  $\tilde{\Pi} = 10$  dBm. User mobility is modeled using the random direction model [43] with speed equal to 3 km/h, for low mobility, and 120 km/h, for high mobility.

To show the impact of a real protocol implementation, the CSI report delay is set to 2 ms. However, the CSI feedback is assumed to be ideal with regard to precision and overhead: the user receives a non-quantized channel gain value for each sub-channel, and no occupation of the downlink channel is considered. Quantization, wideband channel status, and downlink occupation can be topics for future research.

To evaluate the behavior of the proposed strategy in different traffic load conditions, the target bit-rates are set to either 300 kb/s or 1000 kb/s per user. When allocating radio resources to a user, the amount of bits to be transmitted during one sub-frame is rounded up to the nearest Transport Block Size (TBS) allowed in LTE.

Each simulation lasts 10 seconds and all the simulation results have been averaged over 25 runs. The 95% confidence interval has been also computed by using the t-Student

Table IV: Average transmission power registered by mobile terminals (mW).

		Number of users					
		5	10	15	20	25	
Target rate	300 kbps	Proportional fair <sup>a</sup>	39.91	19.96	13.30	9.98	7.98
		Multi-user mMIMO <sup>a</sup>	209.53	209.53	209.53	209.53	209.53
		Proposal <sup>b</sup>	10.39	10.45	10.74	10.90	11.03
	1000 kbps	Proposal <sup>c</sup>	10.42	10.55	10.76	10.86	10.92
		Proportional fair <sup>a</sup>	39.91	19.96	13.30	9.98	7.98
		Multi-user mMIMO <sup>a</sup>	209.53	209.53	209.53	209.53	209.53
	Proposal <sup>b</sup>	11.85	12.49	13.20	13.35	13.73	
	Proposal <sup>c</sup>	11.97	12.36	12.84	13.07	13.30	

<sup>a</sup> for 3 km/h and 120 km/h.

<sup>b</sup> for 3 km/h.

<sup>c</sup> for 120 km/h.

statistic. However, it has not been included in all the graphs because its value is lower than the marker size. All simulation parameters are summarized in Table III.

## B. Results

The set of metrics measured for the performance evaluation include: average per-user transmission power, average power consumption at the base station, average per-user energy efficiency, average MCS used for the transmission, average number of sub-channels that each user selects for transmitting application data, average application goodput experienced by each user during the simulation, peak data rate, system spectral efficiency, and average outage probability.

1) *Power consumptions and energy efficiency*: The average power consumption measured by mobile terminals is reported in Table IV. With multi-user mMIMO, users always consume the maximum power value  $P_M$  during every time slot. Therefore, the highest power consumption is registered and that value is not influenced by any simulation parameter. On the contrary, proportional fair guarantees a power consumption that decreases as the network load becomes higher, and remains constant with respect to target data rate and users' speed. In this case, each mobile terminal adopts a power level of  $P_M$  when it is scheduled, and 0 otherwise. As a result, the number of time slots that each user may spend for the transmission, and therefore the overall power consumption, decreases when the number of users attached to the base station grows. The designed algorithm always registers the lowest power consumption. In particular, it can be observed that the power consumption grows with the required bit-rate, because each user targets a higher SINR to increase its physical data rate. Similarly, to compensate for the additional multi-user interference in highly loaded scenarios, a higher power consumption is observed. Moreover, the impact of user speed on the power consumption is generally very low.

Even if base stations are generally connected to the power grid (and therefore they are not inherently power-limited), they are responsible for about 90% of the amount of energy spent for running a cellular network. Thus, the reduction of their power demands could be very relevant from an environmental and economic perspective. For this reason, the power consumption occurring at the base station side is also calculated,

Table V: Average power consumption registered by the base station (W).

	Number of users				
	5	10	15	20	25
Proportional fair <sup>a</sup>	2008.52	2061.24	2118	2178	2242.12
Multi-user mMIMO <sup>a</sup>	2056.88	2277.56	2726.24	3517.28	4762.36
Proposal@300 kbps <sup>a</sup>	1980.6	2044.7	2116.4	2185.4	2259.9
Proposal@1000 kbps <sup>a</sup>	2002.7	2070.5	2070.5	2227.8	2331.2

<sup>a</sup> for both 3 km/h and 120 km/h.

by means of the analytical model presented in [44]. This model has been formulated for the conventional MIMO transmission scheme. It has been extended to mMIMO by assuming that the percentage of the power consumption related to the radio-frequency chain and baseband processing is proportional to the number of physical antennas and the number of active MIMO streams, respectively. Results are reported in Table V. As expected, the base station power consumption is not influenced by the users' speed, because the amount of executed operations remains the same. Moreover, it emerges that multi-user mMIMO brings to the highest base station power consumption. In fact, it is in charge to address the highest computational load due to the multi-user decoding (note that the base station power consumption significantly increases with the number of users). On the contrary, proportional fair and the proposed approach just register a base station power consumption that slowly increases with the number of users. In this case, the incremental computational load refers to the processing of downlink communications (that increases with the network load).

Finally, the energy efficiency is a valid metric to demonstrate how energy is effectively used during the transmission. It is obtained as the ratio of the achieved per-user bit-rate and the corresponding transmission power. Fig. 3 shows that proportional fair algorithm ensures an energy efficiency that increases with the network load, because each user transmits for a lower fraction of time and the average power is proportionally lower. On the contrary, multi-user mMIMO always registers the lowest energy efficiency, because the maximum power is employed for all the time. With the proposed scheme, instead, the energy efficiency slightly decreases with the number of users, mostly because higher power levels are progressively needed to meet the QoS constraints. Anyway, it is important to remark that our approach guarantees the highest energy efficiency in most of the investigated scenarios. This result well confirms the respect of its design criteria (i.e., the minimization of the energy consumption). Note that proportional fair registers better results only in a scenario with the highest amount of users and the target data rate set to 300 kbps. However, other results below will demonstrate that this gain is not significant because proportional fair will always register lower user experience data rate, cell throughput, and spectral efficiency.

## 2) Physical transmission settings and bandwidth usage:

Table VI reports the average MCS index selected by mobile users. As widely recognized, the MCS is selected by the link adaptation process as a function of the quality of the

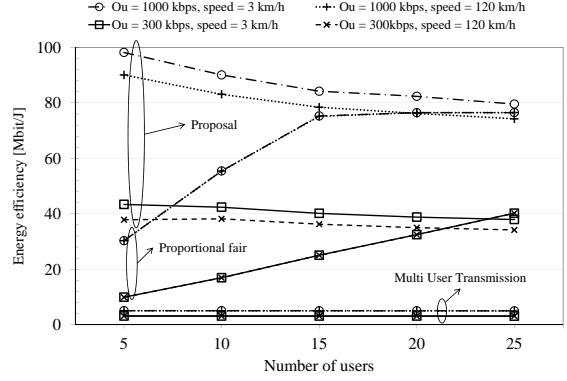


Fig. 3: Average energy efficiency.

communication link, expressed through the SINR. From one side, the worse the channel condition, the lower the MCS index. From another hand, low transmission power and high interference level generally translate to lower MCS indexes. Now, higher user speeds brings to a worse channel quality. Indeed, users moving at 120 km/h tend to select lower MCS indexes. With proportional fair, users select the highest MCS indexes. In fact, they experience the best channel condition because of the absence of intra-cell interference and the use of the maximum power level. Reported results seem to be independent from the network load, the traffic load and the user speed. Only few statistical variations, due to the variability of the channel quality and the user position, are measured. Intra-cell interference, instead, exists for both multi-user mMIMO and the proposed solution. For this reason, they register a lower average MCS index, that also decreases with the network load (because of the increment of the interference level). When multi-user mMIMO is used, a constant power profile is always used and the resulting average MCS index does not change with the target user data rate. The proposed solution, however, generally registers the lowest average MCS index. This result can be justified by considering that the formulated algorithm tries to cut down the transmission power, thus generating communication links with lesser quality. At the same time, a higher traffic load produces higher interference levels, which entail, in turn, the selection of a lower MCS index.

To provide a further insight on transmission settings, Table VII shows the average number of sub-channels assigned to (or selected by) a user in every time slot. With proportional fair, each user transmits over the entire operative bandwidth only when scheduled and the average number of used sub-channels decreases as the network load increases. Of course, such values do not depend on the target data rate and the users' speed. When multi-user mMIMO is used, all users transmit over the entire bandwidth and the number of sub-channels is always equal to 25. The proposed algorithm reaches different results: the number of sub-channels selected for the transmission is highly influenced by network conditions. For lower network and traffic loads, a limited amount of bandwidth is required to drain the amount of data generated at the

Table VI: Average MCS selected by mobile terminals.

		Number of users				
		5	10	15	20	25
300 kbps	Proportional fair (for 3 km/h)	25.08	25.23	25.23	25.33	25.34
	Multi-user mMIMO (for 3 km/h)	19.41	18.06	16.37	15.09	13.54
	Proposal (for 3 km/h)	18.38	18.42	16.43	15.02	14.17
1000 kbps	Proportional fair (for 3 km/h)	25.08	25.23	25.23	25.33	25.34
	Multi-user mMIMO (for 3 km/h)	19.41	18.06	16.37	15.09	13.54
	Proposal (for 3 km/h)	16.44	14.43	13.50	13.23	12.76
300 kbps	Proportional fair (for 120 km/h)	24.75	24.81	24.59	24.98	24.90
	Multi-user mMIMO (for 120 km/h)	19.10	16.95	14.81	13.02	11.39
	Proposal (for 120 km/h)	17.40	16.62	14.80	14.08	13.67
1000 kbps	Proportional fair (for 120 km/h)	24.75	24.81	24.59	24.98	24.90
	Multi-user mMIMO (for 120 km/h)	19.10	16.95	14.81	13.02	11.39
	Proposal (for 120 km/h)	14.73	13.59	12.72	12.51	12.25

Table VII: Average number of sub-channels per time slot.

		Number of users				
		5	10	15	20	25
300 kbps	Proportional fair <sup>a</sup>	5	2.5	1.66	1.25	1
	Multi-user mMIMO <sup>a</sup>	25	25	25	25	25
	Proposal <sup>b</sup>	1.53	1.53	1.84	2.12	2.29
	Proposal <sup>c</sup>	1.57	1.71	2.01	2.18	2.28
1000 kbps	Proportional fair <sup>a</sup>	5	2.5	1.66	1.25	1
	Multi-user mMIMO <sup>a</sup>	25	25	25	25	25
	Proposal <sup>b</sup>	4.84	5.70	6.25	6.37	6.65
	Proposal <sup>c</sup>	5.33	5.85	6.30	6.46	6.62

<sup>a</sup> for 3 km/h and 120 km/h.

<sup>b</sup> for 3 km/h.

<sup>c</sup> for 120 km/h.

application layer. When the number of users, the target data rate, and the user speed increase, the overall channel conditions decreases (see the comments already provided for the average MCS index) and a higher amount of sub-channels is needed to deliver data. It is important to highlight, however, that the proposed scheme tries to reduce the percentage of bandwidth used by each mobile terminal towards the minimum value that guarantees the respect of the QoS constraints.

3) *User goodput, spectral efficiency, and peak data rate:* The average application goodput is depicted in Fig. 4. It is evident that proportional fair is not able to reach QoS constraints when the base station is called to serve a higher number of users. When the network load increases, in fact, each user can employ fewer time slots for transmitting application data and too many users may violate their QoS constraint. Multi-user mMIMO always exceeds QoS requirements. When  $O_u = 300$  kbps, for instance, mobile terminals can transmit more data than requested because they can always transmit over the entire available bandwidth, by using the maximum allowed transmission power. This performance gain is reached, however, at the cost of an excessive reduction of the energy efficiency. On the other side, the proposed algorithm generally achieves an average user goodput close to the target one, thus demonstrating its ability to adapt transmission settings and reduce energy efficiency, while respecting QoS requirements.

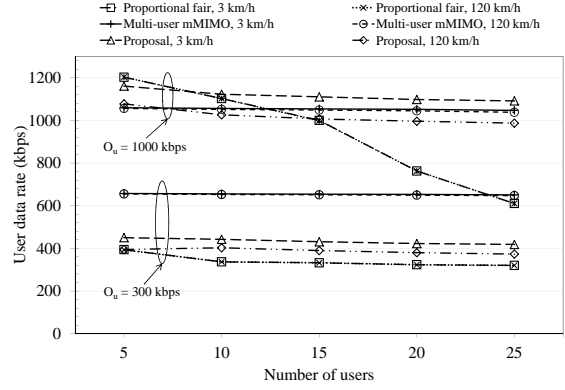


Fig. 4: Average application goodput.

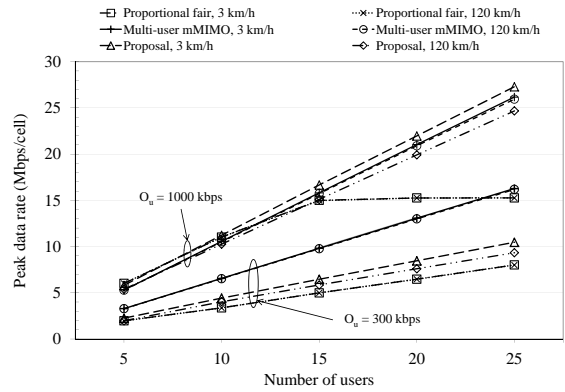


Fig. 5: Peak data rate per cell.

Mobile operators are also interested in the peak data rate achieved in a given cell. This parameter is depicted in Fig. 5. All the results are in line with those just discussed: multi-user mMIMO and the proposed solution register a peak data rate that increases with the number of users. proportional fair, however, achieves worse performance (note that when  $O_u = 1000$  kbps, the peak data rate saturates at about 15 Mbps/cell).

Fig. 6 shows the spectral efficiency, calculated as the ratio of the aggregate transmission bit-rate and the total occupied bandwidth. Also in this case, results confirm the good performance reached by the proposed resource allocation scheme, which always registers higher spectral efficiency when compared with the baseline proportional fair scheme. Similar (or sometimes better) results are measured for the multi-user mMIMO. An interesting behavior is observed for the proposed scheme with  $O_u = 300$  kbps. With a low number of users (up to 15) the spectral efficiency is approximately flat, indicating that a constant number of sub-channels is assigned to each user and they do not overlap. The spectral efficiency is calculated over the *actually allocated* sub-channels, so it remains constant as long as there are free sub-channels to employ when the number of users is raised. Instead, with more than 15 users, the spectral efficiency increases because the number of required sub-channels is greater than the available amount. In fact, they begin to overlap in the frequency domain,

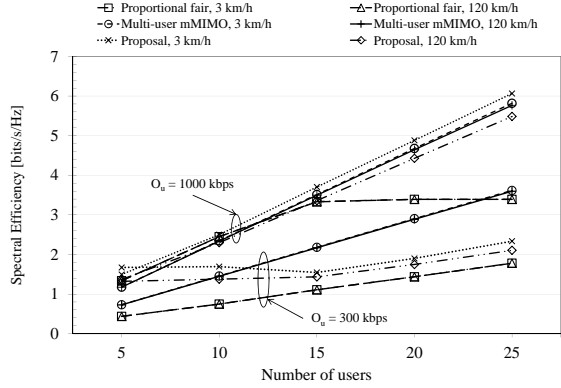


Fig. 6: Average spectral efficiency.

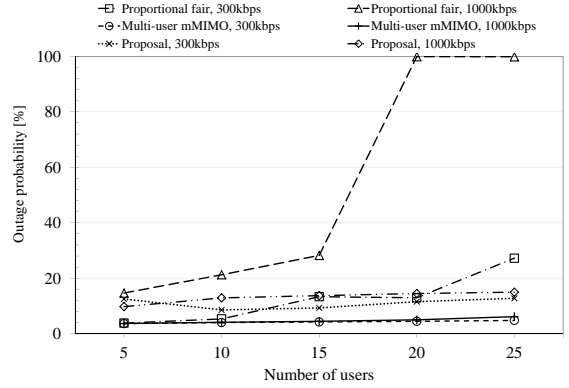


Fig. 8: Outage probability (120 km/h user speed).

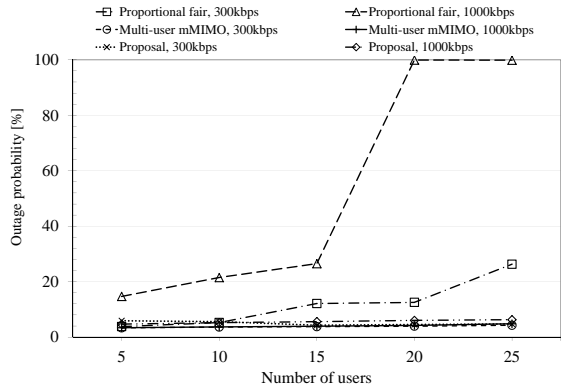


Fig. 7: Outage probability (3 km/h user speed).

but the total number of sub-channels used to calculate the spectral efficiency remains constant while the total goodput grows. This confirms that our proposal guarantees an efficient allocation of the available sub-channels, and the overlapping of different users is avoided if possible.

4) *Outage probability*: To conclude, also the outage probability (see Figs. 7 and 8) has been evaluated, by taking the percentage of time in which a user transmits at a bit-rate lower than the target one. This is the most important performance index that effectively highlights the capability of a given access scheme to satisfy users requirements. Obtained results clearly demonstrate that the proposed approach always reaches a low outage probability (better than round-robin and comparable to multi-user mMIMO).

## V. CONCLUSION

This paper presents a decentralized and scalable radio resource allocation scheme for the uplink of a cellular system, built on top of a physical layer based on the mMIMO transmission scheme and aiming at maximizing the energy efficiency, while guaranteeing the respect of Quality of Service and transmission power constraints. Its effectiveness has been evaluated using computer simulations, through the LTE-Sim tool. The comparison with respect to other baseline approaches is presented too. Obtained results clearly demonstrate that the

developed solution outperforms the other strategies. In fact, it is able to minimize energy consumption at both mobile terminal and base station, optimize transmission settings and bandwidth usage, as well as ensure satisfactory performance in terms of user goodput, peak data rate, spectral efficiency, and outage probability. Therefore, it emerges as a promising solution to be integrated in the upcoming 5G air interface. Future directions for this work will try to extend the applicability of the present framework, including i) the evaluation of performance degradation due to imperfect and limited feedback from the base stations, ii) the analysis of the cost efficiency, and iii) the formulation of the expected performance of the system as a function of the relevant network parameters, that can be highly beneficial for service providers' and network designers' point of view. Moreover, the joint impact that uplink and downlink transmissions, computational load, screen, and other energy-consuming components, have on the battery life of mobile terminals will be investigated too.

## ACKNOWLEDGMENTS

This work is supported by the FANTASTIC-5G project, which receives funding from the European Unions Horizon 2020 research and innovation programme under the grant agreement ICT-671660.

## APPENDIX

This appendix provides details related to the calculation of  $\lambda_{i,u}^a$ ,  $\lambda_{i,u}^b$ , and  $\lambda_{i,u}^c$  variables.

It is assumed that at the  $i$ -th TTI the mobile terminal  $u$  received from the base station a set of SINR values  $\Gamma_{i-\tau,u}(b)$  for each sub-band  $b$ , and the corresponding channel gain values  $\mu_{i-\tau,u,b}$  are evaluated as:

$$\mu_{i-\tau,u}(b) = \frac{\Gamma_{i-\tau,u}(b)}{\Pi_{i-\tau,u}(b)}$$

Among all the estimated channel gains, for the discussion here reported, it is useful to calculate the maximum value,  $\mu_{i,u}^+$ , that is:

$$\mu_{i,u}^+ = \max\{\mu_{i-\tau,u}(b)\} \quad \forall b \in \mathcal{B}$$

Moreover, in the evaluation, non-trivial functions are exploited:

- $\text{rand}()$  is a function which returns a random number in the range  $[0, 1]$  with uniform probability distribution.
- $\text{EESM}(\cdot)$  calculates the exponential effective SINR of the input values, as in (9).
- $\text{MCS}(\cdot)$  maps the effective SINR value to an appropriate MCS index, as in [41].
- $\text{TBS}(m, n)$  returns the TBS, i.e, the size of a data block based on the selected MCS  $m$  and the number of sub-channels  $n$ , as described in the LTE-A specifications [8].

Most symbols which appear in the reported pseudo-code are already defined in Table II. The additional symbols are:

- $\epsilon$ , used as the tolerance to check the convergence of the algorithms
- $\tilde{C}$ , used to calculate and store the estimated channel capacity
- $\tilde{\Omega}$ , used to calculate and store the estimated power consumption
- $\delta$ , which is the objective function that should converge to 0 (described in detail for each algorithm).

#### A. Calculation of $\lambda_{i,u}^a$

Algorithm 1 is used to calculate the energy-efficient water level. As proven in [26], it can be calculated as the root of the function  $\delta = \tilde{C} - \lambda_{i,u}^a \tilde{\Omega}$  [45] where the power levels  $\Pi_{i,u}(b)$  are computed using the WF formula reported in (5). The Dinkelbach's numerical method [46] is used to find the desired value iteratively.

The first *repeat-until* loop determines a suitable initial value to initialize the algorithm, so that  $\delta > 0$  holds. Whereas in [26] many random values are tried until this condition is met, here it can be observed that the useful range for  $\lambda_{i,u}^a$  spans from 0 (which is the limit case when an infinite power level is used) to  $\mu_{i,u}^+$  (which is the limit case where no power is used because  $1/\lambda_{i,u}^a - 1/\mu_{i-\tau,u}(b) < 0 \forall b \in \mathcal{B}$ ). Therefore, a random number is picked from this interval and then decreased multiple times until  $\delta > 0$ . In particular, a small enough value for  $\lambda_{i,u}^a$  is adopted to correctly initialize the algorithm. To prove the effectiveness of this procedure, it is sufficient to show that when  $\lambda_{i,u}^a \rightarrow 0^+$  then  $\delta \rightarrow +\infty$ , that is  $\delta$  remains positive when  $\lambda_{i,u}^a$  approaches 0 from above. In fact, by definition  $\delta = \tilde{C} - \lambda_{i,u}^a \tilde{\Omega}$ , that is:

$$\delta = \sum_{b=0}^{B-1} \log_2 [1 + \mu_{i-\tau,u}(b) \Pi_{i,u}(b)] - \lambda_{i,u}^a \left( \tilde{\Pi} + \sum_{b=0}^{B-1} \Pi_{i,u}(b) \right). \quad (12)$$

Hence

$$\delta = \sum_{b=0}^{B-1} \log_2 \left[ 1 + \mu_{i-\tau,u}(b) \max \left\{ \frac{1}{\lambda_{i,u}^a} - \frac{1}{\mu_{i-\tau,u}(b)}, 0 \right\} \right] - \lambda_{i,u}^a \left[ \tilde{\Pi} + \sum_{b=0}^{B-1} \max \left\{ \frac{1}{\lambda_{i,u}^a} - \frac{1}{\mu_{i-\tau,u}(b)}, 0 \right\} \right]. \quad (13)$$

Now, taking the limit for  $\lambda_{i,u}^a \rightarrow 0^+$ , the quantity:

$$\frac{1}{\lambda_{i,u}^a} - \frac{1}{\mu_{i-\tau,u}(b)} \quad (14)$$

goes to infinity. Therefore, the expression:

$$\max \left\{ \frac{1}{\lambda_{i,u}^a} - \frac{1}{\mu_{i-\tau,u}(b)}, 0 \right\} \quad (15)$$

always reduces to (14), i.e. all sub-channels become active. Exploiting this fact, (13) simplifies as follows:

$$\begin{aligned} \lim_{\lambda_{i,u}^a \rightarrow 0^+} \delta &= \\ &= \lim_{\lambda_{i,u}^a \rightarrow 0^+} \sum_{b=0}^{B-1} \log_2 \left[ 1 + \mu_{i-\tau,u}(b) \left( \frac{1}{\lambda_{i,u}^a} - \frac{1}{\mu_{i-\tau,u}(b)} \right) \right] \\ &- \lim_{\lambda_{i,u}^a \rightarrow 0^+} \lambda_{i,u}^a \left[ \tilde{\Pi} + \sum_{b=0}^{B-1} \left( \frac{1}{\lambda_{i,u}^a} - \frac{1}{\mu_{i-\tau,u}(b)} \right) \right]. \quad (16) \end{aligned}$$

After some derivations, we obtain:

$$\begin{aligned} \lim_{\lambda_{i,u}^a \rightarrow 0^+} \delta &= \lim_{\lambda_{i,u}^a \rightarrow 0^+} \sum_{b=0}^{B-1} \log_2 \left[ \frac{\mu_{i-\tau,u}(b)}{\lambda_{i,u}^a} \right] \\ &- \lim_{\lambda_{i,u}^a \rightarrow 0^+} \left\{ \lambda_{i,u}^a \tilde{\Pi} - \sum_{b=0}^{B-1} \left[ 1 - \frac{\lambda_{i,u}^a}{\mu_{i-\tau,u}(b)} \right] \right\} = +\infty. \quad (17) \end{aligned}$$

Hence, when  $\lambda_{i,u}^a$  is small enough,  $\delta$  is positive and the algorithm could be correctly initialized.

The second *repeat-until* loop is the Dinkelbach's algorithm used to calculate the sequence of values for  $\lambda_{i,u}^a$  converging to the desired value. At each iteration  $\lambda_{i,u}^a$  is updated according to:

$$\delta = \tilde{C} - \lambda_{i,u}^a \tilde{\Omega} = 0, \quad (18)$$

that is:

$$\lambda_{i,u}^a = \tilde{C} / \tilde{\Omega}. \quad (19)$$

Then, the convergence is checked, exiting from the loop if the target condition is met (within a given tolerance  $\epsilon$ ).

Observe that at time instant  $i$  the channel gains  $\mu_{i-\tau,u}(b)$  are related to a previous instant  $i - \tau$  in time, to account for the CQI aging effect.

#### B. Calculation of $\lambda_{i,u}^b$

Algorithm 2 is used to find the water level that minimizes the power required for the target bit-rate. This is known in the literature as the Inverse WaterFilling (IWF) problem [47].

In this case, a simple bisection-based numerical approach is applied. More advanced methods are difficult to implement because the target function (i.e., the TBS) does not have an analytical expression. Instead, it is provided through look-up tables defined by LTE-A specifications [8].

The useful search range, delimited by  $[\lambda^-, \lambda^+]$ , is initially set to  $[0, \mu_{i,u}^+]$ , similarly to Algorithm 1. At each step, the mean value is calculated and checked for convergence. As

---

**Algorithm 1** Calculation of  $\lambda_{i,u}^a$ .

---

```
1: Set  $\epsilon = 10^{-4}$ ;  
2: Set  $\lambda_{i,u}^a = 10 \cdot \text{rand}() \cdot \mu_{i,u}^+$   
   {initialization phase}  
3: repeat  
4:    $\lambda_{i,u}^a = 0.1 \cdot \lambda_{i,u}^a$   
5:    $\tilde{\Omega} = \tilde{\Pi}$   
6:    $\tilde{C} = 0$   
7:   for  $b = 0; b < B; b = b + 1$  do  
8:      $\Pi_{i,u}(b) = \max \left\{ 1/\lambda_{i,u}^a - 1/\mu_{i-\tau,u}(b), 0 \right\}$   
9:      $\tilde{\Omega} = \tilde{\Omega} + \Pi_{i,u}(b)$   
10:     $\tilde{C} = \tilde{C} + \log_2(1 + \mu_{i-\tau,u}(b)\Pi_{i,u}(b))$   
11:   end for  
12:    $\delta = \tilde{C} - \lambda_{i,u}^a \tilde{\Omega}$   
13: until  $\delta > 0$   
   {convergence phase}  
14: repeat  
15:    $\tilde{\Omega} = \tilde{\Pi}$   
16:    $\tilde{C} = 0$   
17:   for  $b = 0; b < B; b = b + 1$  do  
18:      $\Pi_{i,u}(b) = \max \left\{ 1/\lambda_{i,u}^a - 1/\mu_{i-\tau,u}(b), 0 \right\}$   
19:      $\tilde{\Omega} = \tilde{\Omega} + \Pi_{i,u}(b)$   
20:      $\tilde{C} = \tilde{C} + \log_2(1 + \mu_{i-\tau,u}(b)\Pi_{i,u}(b))$   
21:   end for  
22:    $\delta = \tilde{C} - \lambda_{i,u}^a \tilde{\Omega}$   
23:    $\lambda_{i,u}^a = \tilde{C}/\tilde{\Omega}$   
24: until  $|\delta| \leq \epsilon$   
25: return  $\lambda_{i,u}^a$ 
```

---

the function  $\text{TBS}(m, n)$  has discrete values, where  $m$  is the selected MCS and  $n$  is the number of active sub-channels,<sup>3</sup> the exit condition from the loop is verified as soon as the TBS calculated with the current MCS (denoted by  $t$ ) is higher than the required value and the TBS with a lower MCS (denoted as  $t'$ ) is lower. If the convergence condition is not met, the upper or the lower half of the search interval is updated for the next iteration. In particular, the lower half (corresponding to higher power levels) is chosen if the estimated TBS is too low, and the upper half (corresponding to lower power levels) is used otherwise. In addition to this, if the effective SINR  $\Gamma_{i,u}^{\text{eff}}$  is lower than a given minimum threshold  $\Gamma_{\min}$ ,<sup>4</sup> the lower half of the search interval is selected.

### C. Calculation of $\lambda_{i,u}^c$

Algorithm 3 is a modified version of Algorithm 1, using the same iterative method but to converge towards the water level  $\lambda_{i,u}^c$  (i.e., it is the solution of the well-known WF problem [47]).

In this case the function which should converge to 0 is the difference between the target power and the actual used power:

$$\delta = \tilde{\Pi} - P_M = 0 \quad (20)$$

The initialization phase is used to look for water level yielding a positive value of  $\delta$ , with the same principle as Algorithm 1.

<sup>3</sup>An active sub-channel  $b$  for user  $u$  at TTI is such that  $\Pi_{i,u}(b) > 0$ .

<sup>4</sup> $\Gamma_{\min}$  is the SINR value corresponding to the lowest MCS, i.e. such that  $\text{MCS}(\Gamma_{\min}) = 0$ . It depends on the physical air interface, and specifically on the SINR-MCS mapping. When  $\Gamma_{i,u}^{\text{eff}} < \Gamma_{\min}$  a reliable communication cannot be achieved.

---

**Algorithm 2** Calculation of  $\lambda_{i,u}^b$ .

---

```
1: Set  $\epsilon = 10^{-4}$ ;  
2: Set  $\lambda^- = 0$   
3: Set  $\lambda^+ = \mu_{i,u}^+$   
4: repeat  
5:    $\lambda_{i,u}^b = (\lambda^+ + \lambda^-)/2$   
6:    $n = 0$   
7:   for  $b = 0; b < B; b = b + 1$  do  
8:      $\Pi_{i,u}(b) = \max \left\{ 1/\lambda_{i,u}^b - 1/\mu_{i-\tau,u}(b), 0 \right\}$   
9:      $\Gamma_{i,u}(b) = \mu_{i-\tau,u}(b) \cdot \Pi_{i,u}(b)$   
10:    if  $\Pi_{i,u}(b) > 0$  then  
11:       $n = n + 1$   
12:    end if  
13:  end for  
14:   $\Gamma_{i,u}^{\text{eff}} = \text{EESM}(\{\Gamma_{i,u}(b), \forall b \in \mathcal{B} : \Gamma_{i,u}(b) > 0\})$   
15:  if  $\Gamma_{i,u}^{\text{eff}} < \Gamma_{\min}$  then  
16:     $\lambda^+ = \lambda_{i,u}^b$   
17:  continue  
18:  end if  
19:   $m = \text{MCS}(\Gamma_{i,u}^{\text{eff}})$   
20:   $t = \text{TBS}(m, n)$   
21:  if  $m > 0$  then  
22:     $t' = \text{TBS}(m - 1, n)$   
23:  else  
24:     $t' = 0$   
25:  end if  
26:  if  $(t \geq R_u) \wedge (t' < R_u)$  then  
27:    break  
28:  end if  
29:  if  $t > R_u$  then  
30:     $\lambda^- = \lambda_{i,u}^b$   
31:  else  
32:     $\lambda^+ = \lambda_{i,u}^b$   
33:  end if  
34: until false  
35: return  $\lambda_{i,u}^b$ 
```

---

For the convergence phase, the update formula for  $\lambda_{i,u}^c$  can be derived by replacing  $\tilde{\Pi}$  using (5):

$$\delta = \sum_{b=0}^{B-1} \max \left\{ \frac{1}{\lambda_{i,u}^c} - \frac{1}{\mu_{i-\tau,u}(b)}, 0 \right\} - P_M = 0. \quad (21)$$

Rearranging (21) yields

$$P_M = \frac{n}{\lambda_{i,u}^c} - \sum_{b \in \mathcal{B}: \mu_{i-\tau,u}(b) > \lambda_{i,u}^c} \frac{1}{\mu_{i-\tau,u}(b)} \quad (22)$$

where  $n$ , introduced in Appendix B, is the number of active sub-channels, i.e., by definition,  $n = |\mathcal{N}|$ , and the subset  $\mathcal{N} \subseteq \mathcal{B}$  is such that  $\mu_{i-\tau,u}(b) > \lambda_{i,u}^c$  for any  $b \in \mathcal{N}$ .

Otherwise stated,

$$\lambda_{i,u}^c = n \left( P_M + \sum_{b \in \mathcal{B}: \mu_{i-\tau,u}(b) > \lambda_{i,u}^c} \frac{1}{\mu_{i-\tau,u}(b)} \right)^{-1}. \quad (23)$$

However, since  $\lambda_{i,u}^c$  is not available for this comparison while it is being calculated, the value from the previous iteration can be used instead.

Please note that, in this case, the power consumption of the electronic components  $\tilde{\Pi}$  is not taken into account, as the limitation is only on the radiated power.

---

**Algorithm 3** Calculation of  $\lambda_{i,u}^c$ .

---

```
1: Set  $\epsilon = 10^{-4}$ ;  
2: Set  $\lambda_{i,u}^c = 10 \cdot \text{rand}() \cdot \mu_{i,u}^+$   
   {initialization phase}  
3: repeat  
4:    $\lambda_{i,u}^c = 0.1 \cdot \lambda_{i,u}^c$   
5:    $\tilde{\Omega} = 0$   
6:   for  $b = 0; b < B; b = b + 1$  do  
7:      $\Pi_{i,u}(b) = \max \left\{ 1/\lambda_{i,u}^c - 1/\mu_{i-\tau,u}(b), 0 \right\}$   
8:      $\tilde{\Omega} = \tilde{\Omega} + \Pi_{i,u}(b)$   
9:   end for  
10:   $\delta = \tilde{\Omega} - P_M$   
11: until  $\delta > 0$   
   {convergence phase}  
12: repeat  
13:   $\sigma = 0$   
14:   $n = 0$   
15:  for  $b = 0; b < B; b = b + 1$  do  
16:    if  $\mu_{i-\tau,u,b} > \lambda_{i,u}^{(3)}$  then  
17:       $\sigma = \sigma + 1/\mu_{i-\tau,u,b}$   
18:       $n = n + 1$   
19:    end if  
20:  end for  
21:   $\lambda_{i,u}^{(3)} = n / (P + \sigma)$   
22:   $\tilde{\Pi} = 0$   
23:  for  $b = 0; b < B; b = b + 1$  do  
24:     $\Pi_{i,u,b} = \max \left\{ 1/\lambda_{i,u}^{(3)} - 1/\mu_{i-\tau,u,b}, 0 \right\}$   
25:     $\tilde{\Pi} = \tilde{\Pi} + \Pi_{i,u,b}$   
26:  end for  
27:   $\delta = \tilde{\Pi} - P$   
28: until  $|\delta| \leq \epsilon$   
29: return  $\lambda_{i,u}^{(3)}$ 
```

---

**REFERENCES**

- [1] Q. Inc., “The 1000x data challenge,” Qualcomm Inc., Tech. Rep., Nov. 2013. [Online]. Available: <http://www.qualcomm.com/1000x>
- [2] 4G Americas, “Meeting the 1000x challenge,” 4G Americas, Tech. Rep., 2014.
- [3] A. Al-Dulaimi, S. Al-Rubaye, Q. Ni, and E. Sousa, “5G Communications Race: Pursuit of More Capacity Triggers LTE in Unlicensed Band,” *IEEE Vehicular Technology Magazine*, vol. 10, no. 1, pp. 43–51, Mar. 2015.
- [4] G. Wu, C. Yang, S. Li, and G. Y. Li, “Recent advances in energy-efficient networks and their application in 5G systems,” *IEEE Transactions on Wireless Communications*, vol. 22, no. 2, pp. 145–151, 2015.
- [5] J. F. Monserrat, G. Mange, V. Braun, H. Tullberg, G. Zimmermann, and Ö. Bulakci, “METIS research advances towards the 5G mobile and wireless system definition,” *EURASIP Journal on Wireless Communications and Networking*, vol. 53, no. 1, pp. 1–16, 2015.
- [6] E. Hossain and M. Hasan, “5G cellular: key enabling technologies and research challenges,” *IEEE Instrumentation & Measurement Magazine*, vol. 18, no. 3, pp. 11–21, 2015.
- [7] L. Liu, R. Chen, S. Geirhofer, K. Sayana, Z. Shi, and Y. Zhou, “Downlink MIMO in LTE-Advanced: SU-MIMO vs. MU-MIMO,” *IEEE Communications Magazine*, vol. 50, no. 2, pp. 140–147, 2012.
- [8] 3GPP, “Evolved Universal Terrestrial Radio Access (E-UTRA); Physical layer procedures,” 3rd Generation Partnership Project (3GPP), TS 36.213, Sep. 2008. [Online]. Available: <http://www.3gpp.org/ftp/Specs/html-info/36213.htm>
- [9] J. Hoydis, S. Ten Brink, and M. Debbah, “Massive MIMO in the UL/DL of cellular networks: How many antennas do we need?” *IEEE Journal on Selected Areas in Communications*, vol. 31, no. 2, pp. 160–171, 2013.
- [10] D. W. K. Ng, E. S. Lo, and R. Schober, “Energy-efficient resource allocation in OFDMA systems with large numbers of base station antennas,” *IEEE Transactions on Wireless Communications*, vol. 11, no. 9, pp. 3292–3304, 2012.
- [11] T. E. Bogale, L. B. Le, and A. Haghighat, “User scheduling for massive MIMO OFDMA systems with hybrid analog-digital beamforming,” in *Proc. of IEEE International Conference on Communications (ICC)*, 2015, pp. 1757–1762.
- [12] H. Huh, S.-H. Moon, Y.-T. Kim, I. Lee, and G. Caire, “Multi-cell MIMO downlink with cell cooperation and fair scheduling: A large-system limit analysis,” *IEEE Transactions on Information Theory*, vol. 57, no. 12, pp. 7771–7786, 2011.
- [13] D. Bethanabhotla, O. Y. Bursalioglu, H. C. Papadopoulos, and G. Caire, “User association and load balancing for cellular massive MIMO,” in *Proc. of IEEE Information Theory and Applications Workshop (ITA)*, 2014, pp. 1–10.
- [14] E. Bjornson, E. G. Larsson, and M. Debbah, “Optimizing multi-cell massive MIMO for spectral efficiency: How many users should be scheduled?” in *Proc. of IEEE Global Conference on Signal and Information Processing (GlobalSIP)*, 2014, pp. 612–616.
- [15] Cisco, “Visual networking index: Global mobile data traffic forecast update, 20152020,” Online: <http://www.cisco.com/c/en/us/solutions/collateral/service-provider/visual-networking-index-vni/mobile-white-paper-c11-520862.pdf>, February 2016.
- [16] FANTASTIC-5G, “Air interface framework and specification of system level simulations D2.1,” 2016.
- [17] C. Zarakovitis and Q. Ni, “Maximising energy efficiency in multi-user multi-carrier broadband wireless systems: convex relaxation and global optimisation techniques,” *IEEE Transactions on Vehicular Technology*, vol. 65, pp. 5275–5286, Jul. 2015.
- [18] C. C. Zarakovitis, Q. Ni, D. E. Skordoulis, and M. G. Hadjinicolaou, “Power-efficient cross-layer design for OFDMA systems with heterogeneous QoS, imperfect CSI, and outage considerations,” *IEEE Transactions on Vehicular Technology*, vol. 61, no. 2, pp. 781–798, 2012.
- [19] Q. Sun, S. Han, I. Chin-Lin, and Z. Pan, “Energy efficiency optimization for fading MIMO non-orthogonal multiple access systems,” in *Proc. of IEEE International Conference on Communications (ICC)*, 2015, pp. 2668–2673.
- [20] Y. Hu, B. Ji, Y. Huang, F. Yu, and L. Yang, “Energy-Efficient Resource Allocation in Uplink Multiuser Massive MIMO Systems,” *International Journal of Antennas and Propagation*, pp. 1–9, 2015.
- [21] K. Guo, Y. Guo, G. Fodor, and G. Ascheid, “Uplink power control with MMSE receiver in multi-cell MU-massive-MIMO systems,” in *Proc. of IEEE International Conference on Communications (ICC)*, 2014, pp. 5184–5190.
- [22] G. Bacci, S. Lasaulce, W. Saad, and L. Sanguinetti, “Game theory for networks: A tutorial on game-theoretic tools for emerging signal processing applications,” *IEEE Signal Processing Magazine*, vol. 33, no. 1, pp. 94–119, 2016.
- [23] Q. Ni and C. C. Zarakovitis, “Nash bargaining game theoretic scheduling for joint channel and power allocation in cognitive radio systems,” *IEEE Journal on Selected Areas in Communications*, vol. 30, no. 1, pp. 70–81, 2012.
- [24] G. Scutari, D. P. Palomar, and S. Barbarossa, “Competitive design of multiuser MIMO systems based on game theory: A unified view,” *IEEE Journal on Selected Areas in Communications*, vol. 26, no. 7, pp. 1089–1103, 2008.
- [25] K. Guo, Y. Guo, and G. Ascheid, “Energy-Efficient Uplink Power Allocation in Multi-Cell MU-Massive-MIMO Systems,” in *Proc. of 21th VDE European Wireless Conference*, 2015, pp. 1–5.
- [26] G. Bacci, E. V. Belmega, P. Mertikopoulos, and L. Sanguinetti, “Energy-Aware Competitive Power Allocation for Heterogeneous Networks Under QoS Constraints,” *IEEE Trans. Wireless Commun.*, vol. 14, no. 9, pp. 4728–4742, Sep. 2015.
- [27] G. Piro, L. A. Grieco, G. Boggia, F. Capozzi, and P. Camarda, “Simulating LTE cellular systems: an open-source framework,” *IEEE Transactions on Vehicular Technology*, vol. 60, no. 2, pp. 498–513, 2011.
- [28] E. Larsson, O. Edfors, F. Tufvesson, and T. Marzetta, “Massive MIMO for next generation wireless systems,” *IEEE Communications Magazine*, vol. 52, no. 2, pp. 186–195, 2014.
- [29] T. L. Marzetta, “Noncooperative cellular wireless with unlimited numbers of base station antennas,” *IEEE Transactions on Wireless Communications*, vol. 9, no. 11, pp. 3590–3600, 2010.
- [30] H. Q. Ngo, E. G. Larsson, and T. L. Marzetta, “Energy and spectral efficiency of very large multiuser MIMO systems,” *IEEE Transactions on Communications*, vol. 61, no. 4, pp. 1436–1449, 2013.
- [31] E. G. Larsson, O. Edfors, F. Tufvesson, and T. L. Marzetta, “Massive MIMO for next generation wireless systems,” *IEEE Signal Processing Magazine*, vol. 52, no. 2, pp. 186–195, Feb. 2014.
- [32] H. Yang and T. L. Marzetta, “Total energy efficiency of cellular large scale antenna system multiple access mobile networks,” in *Proc. of IEEE Online Conference on Green Communications (GreenCom)*, 2013, pp. 27–32.

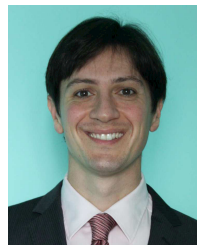
- [33] D. Ha, K. Lee, and J. Kang, "Energy efficiency analysis with circuit power consumption in massive MIMO systems," in *Proc. of IEEE 24th International Symposium on Personal Indoor and Mobile Radio Communications (PIMRC)*, 2013, pp. 938–942.
- [34] E. Bjornson, L. Sanguinetti, J. Hoydis, and M. Debbah, "Designing multi-user MIMO for energy efficiency: When is massive MIMO the answer?" in *Proc. of IEEE Wireless Communications and Networking Conference (WCNC)*, 2014, pp. 242–247.
- [35] E. Bjornson, J. Hoydis, M. Kountouris, and M. Debbah, "Massive MIMO systems with non-ideal hardware: Energy efficiency, estimation, and capacity limits," *IEEE Transactions on Information Theory*, vol. 60, no. 11, pp. 7112–7139, 2014.
- [36] F. Capozzi, G. Piro, L. A. Grieco, G. Boggia, and P. Camarda, "Downlink Packet Scheduling in LTE Cellular Networks: Key Design Issues and a Survey," *IEEE Commun. Surveys and Tutorials*, vol. 15, no. 2, pp. 678–700, Apr. 2013.
- [37] N. Abu-Ali, A.-E. Taha, M. Salah, and H. Hassanein, "Uplink Scheduling in LTE and LTE-Advanced: Tutorial, Survey and Evaluation Framework," *IEEE Commun. Surveys and Tutorials*, vol. 16, no. 3, pp. 1239–1265, 2014.
- [38] G. Bacci, L. Sanguinetti, and M. Luise, "Understanding game theory via wireless power control," *IEEE Signal Processing Magazine*, vol. 32, no. 4, pp. 132–137, Jul. 2015.
- [39] F. Facchinei and C. Kanzow, "Generalized Nash equilibrium problems," *4OR*, vol. 5, no. 3, pp. 173–210, 2007.
- [40] J. Olmos, S. Ruiz, M. García-Lozano, and D. Martín-Sacristán, "Link abstraction models based on mutual information for LTE downlink," in *COST*, vol. 2100, 2010, pp. 1–18.
- [41] G. Piro, A. Orsino, C. Campolo, G. Araniti, G. Boggia, and A. Molinaro, "D2D in LTE vehicular networking: system model and upper bound performance," in *Proc. of IEEE International Congress on Ultra Modern Telecommunications and Control Systems*, Oct 2015.
- [42] 3GPP, "Physical layer aspect for evolved Universal Terrestrial Radio Access (UTRA)," 3rd Generation Partnership Project (3GPP), TR 25.814, Oct. 2006. [Online]. Available: <http://www.3gpp.org/ftp/Specs/html-info/25814.htm>
- [43] T. Camp, J. Boleng, and V. Davies, "A survey of mobility models for ad hoc network research," *Wireless communications and mobile computing*, vol. 2, no. 5, pp. 483–502, 2002.
- [44] C. Desset, B. Debaillie, V. Giannini, A. Fehske, G. Auer, H. Holtkamp, W. Wajda, D. Sabella, F. Richter, M. J. Gonzalez *et al.*, "Flexible power modeling of LTE base stations," in *Proc. of IEEE Wireless Communications and Networking Conference (WCNC)*, 2012, pp. 2858–2862.
- [45] C. Isheden, Z. Chong, E. Jorswieck, and G. Fettweis, "Framework for link-level energy efficiency optimization with informed transmitter," *IEEE Transactions on Wireless Communications*, vol. 11, no. 8, pp. 2946–2957, 2012.
- [46] W. Dinkelbach, "On nonlinear fractional programming," *Management Science*, vol. 13, no. 7, pp. 492–498, 1967.
- [47] S. Boyd and L. Vandenberghe, *Convex optimization*. Cambridge university press, 2004.



**Alessandro Grassi** (S'16) is a Ph.D. student in information engineering at "Politecnico di Bari", Italy. He received a first level degree in electronics engineering in 2012 and a second level degree (cum laude) in telecommunications engineering in 2015. His research interests include 4G and 5G cellular networks, scheduling and QoS optimization in wireless networks, broadcasting in cellular networks, MIMO and Massive MIMO techniques, and random access protocols for cellular machine-to-machine communications. He is a core developer of the LTE-Sim simulator and he is currently involved in the EU Horizon-2020 project "FANTASTIC-5G".



**Giuseppe Piro** (S'10 – M'13) is an Assistant Professor at "Politecnico di Bari", Italy. He received a first level degree and a second level degree (both cum laude) in Telecommunications Engineering from "Politecnico di Bari", Italy, in 2006 and 2008, respectively. He received the Ph.D. degree in Electronic Engineering from "Politecnico di Bari", Italy, on March 2012. His main research interests include quality of service in wireless networks, network simulation tools, 4G and 5G cellular systems, Information Centric Networking, nano communications, and Internet of Things. He founded both LTE-Sim and NANO-SIM projects and is a developer of Network Simulator 3. He is currently involved in the following EU H2020 projects: FANTASTIC-5G, BONVOYAGE, symbIoTe. He is also regularly involved as member of the TPC of many prestigious international conferences.



**Giacomo Bacci** (S'07 – M'09) received the B.E. and the M.E. degrees in telecommunications engineering and the Ph.D. degree in information engineering from the University of Pisa, Pisa, Italy, in 2002, 2004, and 2008, respectively. In 2006-07, he was a visiting student research collaborator at Princeton University, Princeton, NJ, USA. In 2008-14, he was a post-doctoral research fellow at the University of Pisa. In 2008-2012, he also joined Wiser srl, Livorno, Italy, as a software engineer, and in 2012-14 he was also enrolled as a visiting postdoctoral research associate at Princeton University. Since 2015, he has joined MBI srl, Pisa, Italy, as a product manager for interactive satellite broadband communications.

Dr. Bacci is the recipient of the FP7 Marie Curie International Outgoing Fellowships for career development (IOF) 2011 GRAND-CRU, and received the Best Paper Award from the IEEE Wireless Commun. and Networking Conference (WCNC) 2013, the Best Student Paper Award from the Intl. Waveform Diversity and Design Conf. (WDD) 2007, and the Best Session Paper at the ESA Workshop on EGNOS Performance and Applications 2005. He is also the recipient of the 2014 URSI Young Scientist Award, and he has been named an Exemplary Reviewer 2012 for IEEE Wireless Communications Letters.



**Gennaro Boggia** (S'99 – M'01 – SM'09) received, with honors, the Dr. Eng. Degree in Electronics Engineering in July 1997 and the Ph.D. degree in Electronics Engineering in March 2001, both from the Politecnico di Bari, Italy. Since September 2002, he has been with the Department of Electrical and Information Engineering at the Politecnico di Bari, Italy, where he is currently Associate Professor. From May 1999 to December 1999, he was visiting researcher at the TILab, TelecomItalia Lab, Italy, where he was involved in the study of the Core Network for the evolution of 3G cellular systems. In 2007, he was visiting researcher at FTW (Vienna), where he was involved in activities on passive and active traffic monitoring in 3G networks. He has authored or co-authored more than 120 papers in international journals or conference proceedings, gaining more than 1000 citations. His research interests span the fields of Wireless Networking, Network Security, Cellular Communication, Information Centric Networking, Internet of Things (IoT), Protocol stacks for industrial applications, Internet measurements, Network Performance Evaluation. He is active in the IETF ICNRG working group and in the IEEE WG 6TiSCH. He is also regularly involved as member of the TPC of many prestigious international conferences. Currently, he serves as Associate Editor for the Springer Wireless Networks journal.